Available online at www.sciencedirect.com
ScienceDirect
International Journal of Pharmaceutics 336 (2007) 166–173
INTERNATIONAL JOURNAL OF PHARMACEUTICS
www.elsevier.com/locate/ijpharm

Pharmaceutical Nanotechnology

Evaluation and modification of *N*-trimethyl chitosan chloride nanoparticles as protein carriers

Fu Chen, Zhi-Rong Zhang *, Yuan Huang **

Key Laboratory of Drug Targeting of Ministry of Education, West China School of Pharmacy, Sichuan University, No. 17, Block 3, Southern Renmin Road, Chengdu 610041, PR China

Received 22 June 2006; received in revised form 1 October 2006; accepted 8 November 2006
Available online 12 November 2006

Abstract

N-Trimethyl chitosan chloride (TMC) nanoparticles were prepared by ionic crosslinking of TMC with tripolyphosphate (TPP). Two model proteins with different p*I* value*s*, bovine serum albumin (BSA, p*I* = 4.8) and bovine hemoglobin (BHb, p*I* = 6.8), were used to investigate the loading and release features of the TMC nanoparticles. TMC samples with different degrees of quaternization were synthesized to evaluate its influence on the physicochemical properties and release profiles of the nanoparticles. Sodium alginate was used to modify the TMC nanoparticles to reduce burst release. The results indicated that the TMC nanoparticles had a high loading efficiency (95%) for BSA but a low one (30%) for BHb. The particle size and zeta potential were significantly affected by the BSA concentration but not by the BHb concentration. Nanoparticles of TMC with a lower degree of quaternization showed an increase in particle size, a decrease in zeta potential and a slower drug-release profile. As for the alginate-modified nanoparticles, a smaller size and lower zeta potential were observed and the burst release of BSA was reduced. These studies demonstrated that TMC nanoparticles are potential protein carriers, and that their physicochemical properties and release profile could be optimized by means of various modifications.

Keywords: *N*-Trimethyl chitosan chloride; Nanoparticles; Protein delivery; In vitro release

1. Introduction

Despite advances in biotechnology that have led to the availability of large numbers of protein drugs, these drugs remain difficult to deliver by routes other than parenteral delivery. Parenteral administration has obvious disadvantages, such as low compliance by patients and a significant transmission of disease caused by unsafe injection practices. There is also the problem of inactivation of the proteins during storage and transport. Recently, alternative methods of administration such as the mucosal route, including nasal, oral and vaginal routes, have been used to avoid such disadvantages. However, the hydrophilicity and high molecular weights of protein drugs have limited their permeation across biological barriers and made them unstable in body fluids due to endogenous processes. Therefore, new approaches that improve the delivery of macromolecular drugs across mucosal tissues need to be adopted (Issa et al., 2005).

Chitosan, the second most abundant polysaccharide in nature, has attracted particular interest as a biodegradable material for mucosal delivery systems. It has showed favorable biological properties (Felt et al., 1998), low toxicity and high susceptibility to biodegradation (Lee et al., 1995; Onishi and Machida, 1999), mucoadhesive properties (Bernkop-Schurch et al., 1998), and an important capacity to enhance drug permeability and absorption at mucosal sites (Artursson et al., 1994; van der Lubben et al., 2003). More importantly, chitosan micro/nanoparticles can be spontaneously formed through ionic gelation using tripolyphosphate as the precipitating agent, so that the use of harmful organic solvents can be avoided during preparation and loading (van der Lubben et al., 2001).

In spite of all its superior properties, chitosan has a major drawback: its solubility is poor above pH 6. At physiological pH, chitosan will lose its capacity to enhance drug permeability and absorption, which can only be achieved in its protonated

* Corresponding author. Tel.: +86 28 85501566; fax: +86 28 85501615.
** Corresponding author. Tel.: +86 28 85501617, fax: +86 28 85501617.
E-mail addresses: zrzzl@vip.sina.com (Z.-R. Zhang), huangyuan0@yahoo.com.cn (Y. Huang).

0378-5173/$ – see front matter © 2006 Elsevier B.V. All rights reserved.
doi:10.1016/j.ijpharm.2006.11.027

form in acidic environments (Kotzé et al., 1999). In contrast, *N*-trimethyl chitosan chloride (TMC), a quaternized chitosan derivative, shows perfect solubility in water over a wide pH range (Domard et al., 1986). It also has bioadhesive properties and enhancement of permeability and absorption in neutral and basic-pH environments (Hamman et al., 2002; van der Merwe et al., 2004a).

Recently, Amidi et al. reported that TMC nanoparticles could be prepared by a mild ionic gelation procedure and proved that they are safe carriers for nasal protein delivery (Amidi et al., 2006). In their study, ovalbumin was adopted as a model protein (which is known to have a low p*I*). Although a high loading efficiency and a burst release (30%) were observed, the effect of the degree of quaternization of TMC on the loading and release properties of the nanoparticles and the feasibility of encapsulating proteins with high p*I* were not reported. Moreover, although there have been some other reports about decreasing the burst release of chitosan nanoparticles, only limited data are available for particular TMC carrier systems. All these problems need to be solved before TMC nanoparticles can be widely used as protein carriers. In our study, the effect of the degree of quaternization of TMC on the loading and release properties of nanoparticles and the feasibility of encapsulating proteins with high p*I* were investigated for the first time. Furthermore, we also tried to decrease the initial burst by alginate modification, a method that has not been reported in the literature on TMC carrier systems.

In order to achieve these goals, two model proteins with similar molecular weight ($M_w = 68,000$ Da) but different p*I* values, bovine serum albumin (BSA, p*I* = 4.8) and bovine hemoglobin (BHb, p*I* = 6.8), were used in various concentrations to investigate the protein loading and release profiles of TMC nanoparticles. The influence of the degree of quaternization of TMC on its physicochemical properties was also investigated. To lower burst release, sodium alginate (SL), which has been widely used to modulate the loading and release properties of encapsulated materials and the physical characteristics of delivery systems (Vandenberg et al., 2001; González-Rodríguez et al., 2002), was chosen to modify the TMC nanoparticles. The properties and protein-release profiles of the modified TMC nanoparticles were also investigated.

2. Materials and methods

2.1. Materials

Chitosan (with 95% degree of deacetylation (DD) and a molecular weight (M_w) of 200 kDa) was used for the synthesis of TMC. Bovine serum albumin (BSA) and bovine hemoglobin (BHb) were purchased from BoAo Biochemical Company (Shanghai, China). Tripolyphosphate (TPP) was obtained from Tianjin Chemical Reagents Company (Tianjin, China). Cibacron brilliant red 3B-A was bought from Sigma (USA). All other chemicals were of reagent grade.

2.2. Synthesis and characterization of TMC

TMC samples with different degrees of quaternization were synthesized according to a previous method (Sieval et al., 1998), with some modifications of the reaction time. Briefly, chitosan was methylated by methyl iodide in a strong base (NaOH) solution at 60 °C for 45 min or 90 min to obtain TMC with different degrees of quaternization. The products were purified by dialysis against water and finally lyophilized. The purified products were then analyzed by ^{1}H NMR spectroscopy (Varia^{UNITY}INOVA-400, USA). The degree of quaternization (DQ) was calculated using the following equation (Thanou et al., 2000):

$$\mathrm{DQ}\ (\%) = \left[\left(\frac{\int \mathrm{TM}}{\int \mathrm{H}}\right) \times \frac{1}{9}\right] \times 100$$

where ∫TM is the integral of the trimethyl amino group (quaternary amino group) peak at 3.3 ppm and ∫H is the integral of the ^{1}H peaks from 4.7 to 5.7 ppm.

2.3. Preparation and modification of TMC nanoparticles

2.3.1. Preparation of TMC nanoparticles

The TMC nanoparticles were prepared by the ionic gelation of TMC with TPP anions. 10 mg of TMC (DQ = 33% or 37%) was dissolved in 5 ml of water. Subsequently, 2 ml of TPP solution with various concentrations (from 0.1 to 0.9 mg/ml) was added drop-by-drop to the above solution under magnetic stirring at room temperature. Protein-loaded TMC nanoparticles were prepared by the same method described above (Method A), except that various amounts (0.5, 1.0, 2.0 or 5.0 mg) of proteins (BSA, BHb) were dissolved in the TMC solution before adding the TPP.

2.3.2. Modification of TMC nanoparticles

Alginate-modified BSA-loaded nanoparticles were prepared by dissolving sodium alginate (0.2, 0.4, 0.6 or 0.8 mg) in 2 ml of TPP (0.6 mg/ml) and then adding it to the TMC solution (Method B). BHb-loaded TMC nanoparticles were also prepared by an adjusted method (Method C): different amounts of BHb (0.5, 1.0, 2.0 or 5.0 mg) were dissolved in TPP solution, then added to the TMC solution.

2.4. Physicochemical characterizations of TMC nanoparticles

2.4.1. pH measurements

The pH values of the aqueous TMC solution (2 mg/ml), aqueous TPP solution (0.6 mg/ml) and non-loaded TMC nanoparticle suspensions were determined using a pHS-3C$^+$ potentio/pH-meter (Fangzhou Tech. Ltd., Chengdu, China).

2.4.2. Colorimetric determination of TMC precipitation efficacy

Non-loaded TMC nanoparticle suspensions were centrifuged at 18,000 × g for 15 min. The free TMC in the clear supernatant was determined by the TMC colorimetric assay method (van der Merwe et al., 2004b). A solution of Cibacron brilliant red 3B-A

was prepared in deionized water, at a concentration of 1.5 mg/ml. Aliquots (5 ml) of the stock solution were made up to 100 ml with 0.1 M phosphate-buffered saline (PBS) at pH 7.4. To prepare the standard curve, a stock solution of TMC was prepared at a concentration of 500 μg/ml. Dilutions were made by pipetting different volumes of the stock solution directly into disposable cuvettes, after which the volume in each cuvette was made up to 600 μl with 0.1 M PBS at pH 7.4. Aliquots of the dye solution (2.4 ml) were added to each cuvette and the absorbance at 570 nm wavelength was recorded immediately with a Cintra 10e UV–vis Spectrometer (GBC Scientific Equipment, Australia). Different standard curves were adopted for TMC samples with different degrees of quaternization. The TMC precipitation efficacy (PE) was calculated as follows:

$$\text{PE}\ (\%) = \frac{\text{total amount of TMC} - \text{free TMC}}{\text{total amount of TMC}} \times 100$$

2.4.3. Particle size, zeta potential and morphology

The size and zeta potential of the TMC nanoparticles were measured with a Malvern Zatesize NanoZS90 (Malvern Instruments Ltd., Malvern, UK). The particle-size distribution of the nanoparticles is reported as a polydispersity index (PDI). All measurements were performed in triplicate. Morphological examination of the nanoparticles was performed by transmission electron microscopy (TEM) (Hitachi H-600, Japan).

2.5. Loading efficiency and loading capacity of TMC nanoparticles

The loading efficiency and capacity of the protein-loaded TMC nanoparticles were determined by separating the nanoparticles from free proteins by centrifugation at 18,000 × *g* for 15 min. The amount of free protein in the supernatant was measured by μBCA protein assay (Merck, Germany). The supernatant of non-loaded TMC (DQ = 33% or 37%) nanoparticle suspension was used as a blank. The loading efficiency and loading capacity of the nanoparticles were calculated as follows:

$$\text{LE}\ (\%) = \frac{\text{total amount of protein} - \text{free protein}}{\text{total amount of protein}} \times 100$$

$$\text{LC}\ (\%) = \frac{\text{total amount of protein} - \text{free protein}}{\text{nanoparticles dry}} \times 100$$

All measurements were performed in triplicate.

2.6. In vitro release of proteins from TMC nanoparticles

2.6.1. Protein stability in release medium

Two milligrams of BSA or BHb were incubated in 5 ml of 0.1 M PBS buffer (pH 7.4) containing 0.05% (w/v) sodium azide as preserving agent at 37 °C under magnetic stirring (100 rpm) for 5 days. At scheduled time intervals, samples were withdrawn and assayed by μBCA protein assay to determine the protein concentration. At the end of the 5th day, the integrity of the proteins was evaluated by SDS-polyacrylamide gel electrophoresis (SDS-PAGE). The proteins underwent electrophoresis in 25% SDS-polyacrylamide gel at 200 V under reducing conditions at 4 °C. After electrophoresis, the protein bands were visualized by staining with Coomassie Blue R-250.

2.6.2. In vitro release

Protein-loaded TMC nanoparticles were separated by centrifugation at 10,000 × *g* and 4 °C on a 10-μl glycerol bed for 15 min. The supernatant was decanted and the nanoparticles were resuspended in 6 ml of 0.1 M PBS (pH 7.4), then kept at 37 °C under magnetic stirring (100 rpm). At different time intervals, 0.5 ml of the suspension was taken and centrifuged (18,000 × *g*, 15 min). The protein concentration in the supernatant was analyzed by μBCA protein assay. The same volume of fresh PBS buffer was added to the release medium to reach the original volume. A sample consisting of only non-loaded TMC nanoparticles resuspended in PBS was used as a blank. All of the experiments were performed in triplicate.

3. Results and discussion

3.1. NMR characterization of TMC and pH measurements

TMC polymers with different degrees of quaternization were synthesized simply by altering the reaction time. Since the amount of TPP had a great influence on physicochemical properties such as particle size and zeta potential, the influence of the degree of quaternization of TMC on the nanoparticles can only be investigated for amounts of TPP in the same range. In the preliminary study, we found that TMC polymers with large differences in their degree of quaternization cannot form nanoparticles in a common range, especilly under preparation condition of pH above 6 in our study (when only the quaternized amines can interact with TPP). Therefore, only polymers with relatively close degrees of quaternization can be selected to form nanoparticles. Interestingly, although the degrees of quaternization of these two polymers were 33% and 37%, the nanoparticles

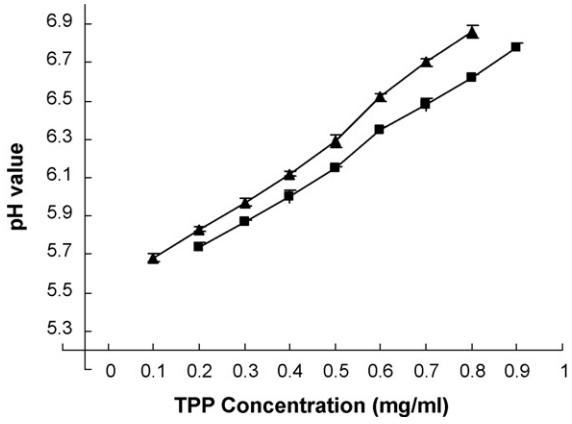

Fig. 1. pH values of TMC nanoparticle suspensions (TMC 2 mg/ml, TPP 0.1–0.9 mg/ml) as a function of TPP concentration. All data are expressed as mean ± S.D. ($n = 3$). TMC33 (▲) and TMC37 (■).

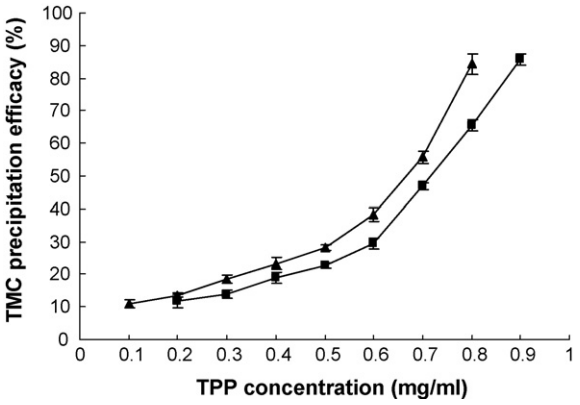

Fig. 2. TMC precipitation efficacy as a function of TPP concentration (TMC 2 mg/ml, TPP 0.1–0.9 mg/ml). Data shown are the mean ± S.D. ($n = 3$). TMC33 (▲) and TMC37 (■).

prepared from these polymers, either with the same or an increased amount of TPP, had large differences in their physico-chemical properties and in vitro release profiles. The pH values of the TMC solutions (2 mg/ml) and nanoparticle suspensions, prepared by adding TPP solutions of different concentrations, are shown in Fig. 1. Nanoparticles could be formed using TPP concentrations of 0.1–0.8 mg/ml for TMC33 and 0.2–0.9 mg/ml for TMC37. Higher TPP concentrations (>0.8 mg/ml for TMC33 and >0.9 mg/ml for TMC37) led to aggregation. The pH value increased from 5.6 to 6.8. TMC37 has a lower pH than TMC33 at any given TPP concentration (0–0.9 mg/ml), probably because of its higher positive charge. This is due to quaternized amines yielding an average charge of ca. +0.37 per amino-sugar unit for TMC37 and ca. +0.33 per amino-sugar unit for TMC33, which makes TMC33 a weaker acid. The pH value of the TPP solution (0.6 mg/ml) was measured to be 9.61.

3.2. Preparation of TMC nanoparticles

3.2.1. Effect of TPP concentration on TMC precipitation efficacy

To study the profile of TMC precipitation with TPP, the effect of TPP concentration on the TMC precipitation efficacy was investigated (Fig. 2). In our experiments, besides tri-methylated (quaternized) amines, mono- and di-methylated amines also existed in the TMC polymers. According to previous work (Amidi et al., 2006; Kotzé et al., 1997), the pK_a values of mono- and di-methylated amines are around 6, which means that all of these amine groups will be ionized and can interact with TPP when the pH of the nanoparticle suspensions is below 6. When more TPP was added, the pH increases. A faster increase of TMC precipitation efficacy was observed for higher TPP concentration (>0.5 mg/ml), with a pH above 6, which might be due to the deionization of the mono- and di-methylated amines of the TMC polymers. Therefore, only the tri-methylated (quaternized) amines can interact with TPP, which led to a higher TMC/TPP (w/w) ratio to form nanoparticles. For the same TPP

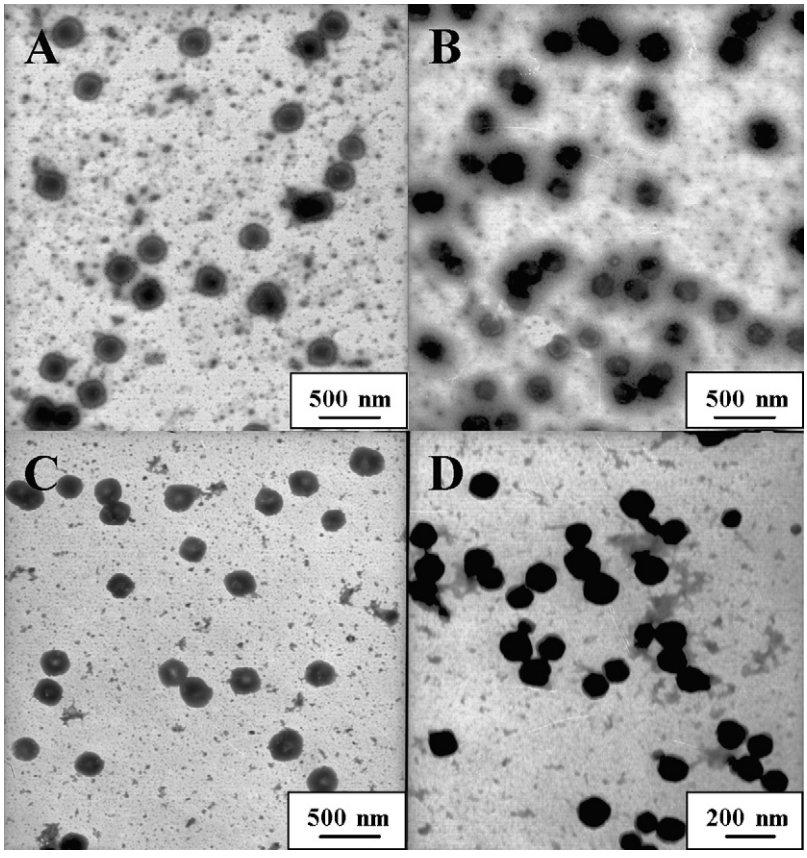

Fig. 3. TEM of non-loaded TMC nanoparticles (A), BSA-loaded TMC nanoparticles (B), BHb-loaded TMC nanoparticles (C) and alginate modified nanoparticles (D). (TMC37 2mg/ml, TPP 0.6 mg/ml, BSA or BHb 0.4 mg/ml, sodium alginate 0.3 mg/ml).

concentration, the precipitation efficacy of TMC33 was higher than that of TMC37, probably because TMC33 has fewer quaternized groups available for interaction with TPP at the same pH value.

3.2.2. TEM characterization of TMC nanoparticles

Fig. 3 shows the morphology of protein-loaded and non-loaded TMC nanoparticles. The nanoparticles observed by TEM have a spherical geometry with a good size distribution.

3.3. Protein loading

3.3.1. Effect of protein concentration on the colloidal properties of TMC nanoparticles

Fig. 4 shows the effect of the BSA or BHb concentration on the particle size and zeta potential of the nanoparticles. As the BSA concentration increased to 1 mg/ml, the particle size gradually increased. This may be ascribed to ionic interaction and ionic cross-linking between negatively charged BSA (pI = 4.8) and positively charged TMC under the preparation conditions (around pH 6). The zeta potential decreased at the same time, which is probably due to the load of negatively charged BSA.

In contrast, the particle size and zeta potential barely changed as the BHb concentration was increased. BHb is known to have a similar molecular weight to BSA (M_w = 68,000 Da) but a higher pI (pI = 6.8). Since the pH of the preparation conditions was around 6.3, the net charge of BHb was close to zero, so there might be some repulsive interaction between BHb and TMC instead of ionic attraction.

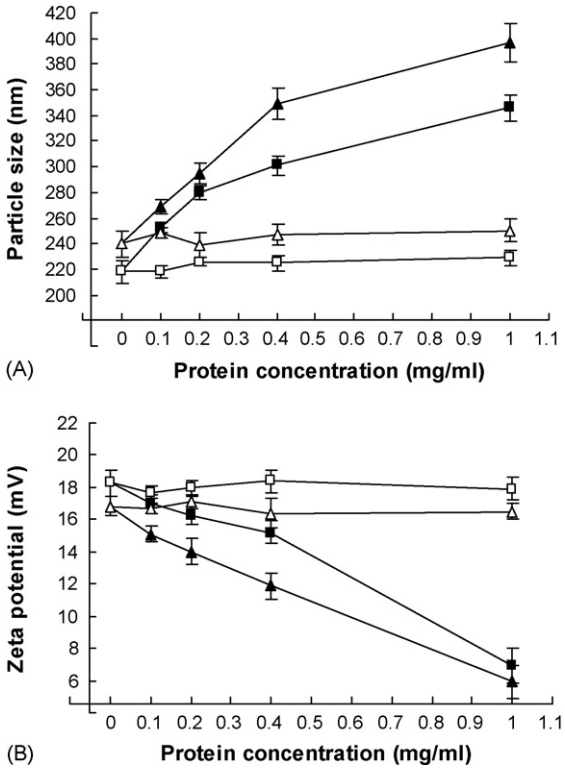

Fig. 4. Particle size (A) and zeta potential (B) of protein-loaded TMC nanoparticles (TMC 2 mg/ml, TPP 0.6 mg/ml) as a function of protein concentration. All data are expressed as mean ± S.D. (n = 3). BSA-loaded TMC33 nanoparticles (▲), BHb-loaded TMC33 nanoparticles (△), BSA-loaded TMC37 nanoparticles (■) and BHb-loaded TMC37 nanoparticles (□).

3.3.2. Effect of protein concentration on loading efficiency and loading capacity of TMC nanoparticles

Table 1 shows the effect of the initial protein concentration on the loading efficiency (LE) and loading capacity (LC) of the TMC nanoparticles. The high loading efficiency of BSA could be due to the ionic interaction between TMC and BSA. Too high a BSA concentration could lead to aggregation. The instability was probably caused by the increase of particle size and the decrease of zeta potential (Fig. 4). To examine further the capacity of the TMC nanoparticles to load BSA, another experiment was carried out in which non-loaded nanoparticles were prepared (TMC37 2 mg/ml, TPP 0.6 mg/ml). After sep-

Table 1
The loading efficiency and loading capacity of TMC nanoparticles (TMC 2 mg/ml, TPP 0.6 mg/ml) loaded with BSA or BHb

Proteins and TMC polymers	Protein concentration (mg/ml)	Loading efficiency (%) (mean ± S.D.) n = 3	Loading capacity (%) (mean ± S.D.) n = 3
BSA/TMC33	0.1	98.40 ± 2.05	10.16 ± 1.17
	0.2	95.49 ± 1.16	19.97 ± 2.13
	0.4	95.57 ± 1.61	40.80 ± 0.44
	1.0	97.71 ± 0.46	59.51 ± 0.50
BSA/TMC37	0.1	97.73 ± 1.86	11.60 ± 2.00
	0.2	96.49 ± 1.16	21.60 ± 0.73
	0.4	95.08 ± 1.17	38.57 ± 0.44
	1.0	98.51 ± 0.44	73.31 ± 1.96
BHb/TMC33	0.1	39.67 ± 1.92	4.72 ± 0.06
	0.2	39.47 ± 2.73	8.96 ± 0.83
	0.4	40.43 ± 1.59	14.49 ± 1.07
	1.0	19.34 ± 1.56	20.05 ± 0.58
BHb/TMC37	0.1	35.52 ± 1.16	4.89 ± 0.04
	0.2	33.66 ± 2.53	8.72 ± 0.38
	0.4	21.84 ± 6.56	11.48 ± 0.92
	1.0	16.86 ± 3.04	19.67 ± 1.42

Table 2
The particles size and zeta potential of TMC nanoparticles (TMC 2 mg/ml, TPP 0.6 mg/ml, BSA or BHb 0.4 mg/ml) prepared by TMC with different degrees of quaternization

Formation	TMC polymers	Particle size (nm) mean ± S.D. ($n = 3$)	PDI	Zeta potential (mV) mean ± S.D. ($n = 3$)
Non-loaded nanoparticles	TMC33	240 ± 10	0.215	16.8 ± 0.6
	TMC37	218 ± 9	0.193	18.3 ± 0.8
BSA-loaded nanoparticles	TMC33	349 ± 12	0.259	11.9 ± 0.8
	TMC37	301 ± 8	0.216	15.2 ± 0.7
BHb-loaded nanoparticles	TMC33	247 ± 8	0.220	15.9 ± 0.9
	TMC37	225 ± 6	0.212	18.4 ± 0.7

aration by centrifugation, these non-loaded nanoparticles were resuspended and incubated with 5 ml BSA solution (0.4 mg/ml) under magnetic stirring. At equilibrium, the BSA concentration in the supernatant was tested by μBCA protein assay. The results showed that as much as 98.88 ± 2.57% of the BSA was loaded into the nanoparticles, indicating that TMC has a high protein-uptake capacity for negatively charged BSA.

However, for nearly uncharged or even positively charged BHb, the LE and LC were much lower than those of BSA (Table 1), indicating that ionic interaction plays an important role in protein loading of TMC nanoparticles.

3.3.3. *Effect of degree of quaternization of TMC on the physicochemical properties of TMC nanoparticles*

As shown in Table 1, the degree of quaternization of TMC had little influence on the BSA loading efficiency and loading capacity, whereas the BHb loading efficiency was improved with a lower degree of quaternization. This is probably because of the higher TMC precipitation efficacy, so that more BHb was loaded with TMC precipitation. The similarity of the BHb loading capacities between TMC33 and TMC37 nanoparticles also supported this viewpoint.

The influence of the degree of quaternization of TMC on the particle size and zeta potential is shown in Table 2. Nanoparticles prepared by TMC33 showed a larger size and PDI, and a lower zeta potential than those prepared with TMC37 for both loaded and non-loaded formations. This may be due to the lower positive charge of TMC33 than TMC37 due to the lower degree of quaternization; thus a less stable gelation system was formed.

3.4. *Effect of TMC nanoparticle modifications*

BSA-loaded TMC nanoparticles were also prepared by modification with sodium alginate (SL) (Method B). Table 3 shows the influence of the SL concentration on LE, particle size, zeta potential and TMC precipitation efficacy. The loading efficiency kept increasing to nearly 100% with increasing SL concentration. This may be because more TMC had gelated into the nanoparticles due to the interaction between the negatively charged COO^- of the alginate and the positively charged $-N^+(CH_3)_3$ of the TMC. The increase of TMC precipitation efficacy with SL concentration supported this assumption. The particle size decreased as more SL was added to the gelation system (Table 3). Since the similarity of the structures of alginate and TMC offered a strong inter-chain reaction between the two polysaccharides, a more compact structure was formed. Other researchers (Aral and Akbuğa, 1998; Xu et al., 2003) have also observed a similar phenomenon. The increase of the PDI might be because more cross-linking agent caused slight local aggregation. The reduction of the zeta potential can be explained by the fact that more anionic polymer (SL) had been cross-linked into the nanoparticles. A high SL concentration (>0.5 mg/ml) could induce large particles and aggregation, probably because of the low particle zeta potential.

To improve further the loading efficiency of BHb, an adjusted method (Method C) was used. BHb was added to TPP solution (pH 9) to achieve a negative net charge before being added to TMC solution. Fig. 5 shows a comparison of the loading efficiencies of BHb nanoparticles prepared by Method A (original method) and Method C (adjusted method) for various BHb concentrations. The results show that the loading efficiency was largely improved from as low as 30% to more than 50% with almost no impact on the particle size and zeta potential (232 ± 12 nm and 18.7 ± 0.4 mV for 2 mg BHb dissolved in TPP solution). It seems that the negative net charge of BHb favors the ionic interaction with TMC.

3.5. *In vitro protein release from TMC nanoparticles*

The results of μBCA protein assay and SDS-PAGE (Fig. 6) show that BSA and BHb were stable in the release medium (0.1 M PBS pH 7.4) for 5 days.

The release profiles of BSA- and BHb-loaded TMC nanoparticles are shown in Fig. 7. An initial burst release of 12–60% was

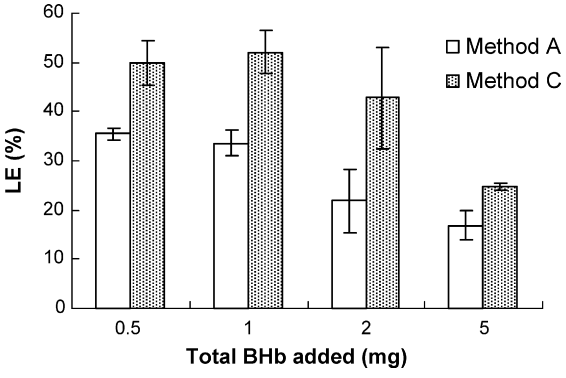

Fig. 5. BHb loading efficiency of nanoparticles (TMC372 mg/ml, TPP 0.6 mg/ml, BHb was either dissolved in TMC solution or TPP solution) prepared by Method A and C. All data are mean ± S.D. ($n = 3$).

Table 3
The loading efficiency, particle size, zeta potential and TMC precipitation efficacy of alginate modified TMC nanoparticles (TMC37 2mg/ml, TPP 0.6 mg/ml, BSA 0.4 mg/ml, SL 0.3 mg/ml)

SL (mg/ml)	Loading efficiency (%)	Particle size (nm)	PDI	Zeta potential (mV)	TMC precipitation efficacy (%)[a]
0	95.08 ± 1.17	301 ± 8	0.216	15.2 ± 0.7	29.52 ± 1.21
0.1	96.46 ± 0.86	232 ± 14	0.193	11.1 ± 0.6	35.89 ± 0.69
0.2	99.16 ± 1.05	201 ± 8	0.217	8.8 ± 0.8	43.29 ± 2.06
0.3	99.4 ± 0.67	175 ± 10	0.230	6.5 ± 0.5	53.83 ± 1.83
0.4	[b]	138 ± 12	0.233	5.0 ± 0.9	56.85 ± 0.96

All data are the mean ± S.D. ($n = 3$).
[a] TMC precipitation efficacy were tested without incorporation of BSA.
[b] Beyond detection limit.

observed in the first 4 h. The burst might be ascribed to protein molecules that were loosely bound with TMC at the particle surface. The much higher burst of BSA than BHb illustrated that protein–polymer binding may play an important role in the initial burst. Since protein had to compete with TPP to bind with TMC during the preparation process, the protein–polymer binding might occur mainly after the nanoparticles were prepared, and thus on the particle surface. In the following 8 h, a reversed release due to the re-adsorption of protein was observed. The re-adsorption was probably due to the increase of specificity of the nanoparticles (Crotts et al., 1997) caused by erosion (polymer degradation) (Bouillot et al., 1999), solubilization (Xu et al., 2003)) or particle swelling (Xu et al., 2003). Although the mechanism of re-adsorption in our experiment is not yet clear, we did observe that nanoparticles prepared from TMC with a high degree of quaternization (89%, prepared by a two-step synthesis according to the literature (Sieval et al., 1998)) dissolved in the release medium immediately, indicating that ionic exchanges between polymer and release medium may lead to solubilization of the reversible physical cross-link of TMC and TPP, which may respond for the re-adsorption. After the re-adsorption, a sustained release continued until the end of the experiment, resulting from the diffusion of drug from the polymer matrix and erosion of the nanoparticles (Bouillot et al., 1999). A long shelf life is very important for protein drugs like vaccines and antibodies. Since traditional vaccines usually require multiple doses to achieve satisfactory protective immunity, sustained release of vaccine drugs can maintain a high antibody level in the lymphatic system, and thus achieve protective immunity with only one dose. Protein was released more slowly from TMC33 nanoparticles than from TMC37 nanoparticles, probably because the lower positively charged TMC33 has a slower ionic exchange between polymer and release medium.

The release profile of modified nanoparticles was also investigated. An important function of mucosal delivery systems is to protect protein drugs from degradation by proteolytic enzymes before they pass through the mucosal epithelium. Therefore, the initial burst of a large amount of protein drug that bound to TMC

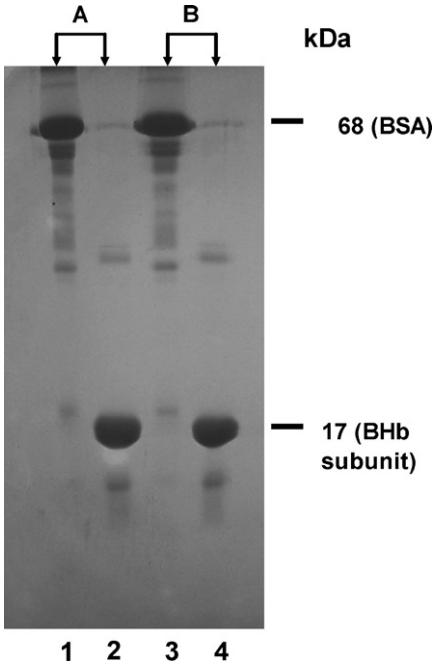

Fig. 6. SDS-PAGE patterns, obtained under reducing conditions, of proteins before (A) and after (B) incubation in release medium. Lanes 1 and 3, BSA; lanes 2 and 4, BHb.

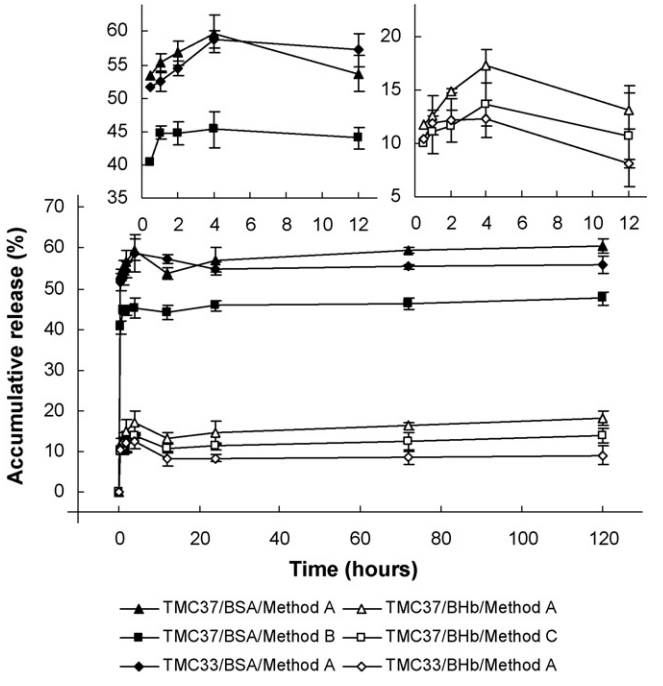

Fig. 7. Release profile of TMC nanoparticles prepared by Method A (TMC 2 mg/ml, TPP 0.6 mg/ml, BSA or BHb 0.4 mg/ml), Method B (TMC372 mg/ml, TPP 0.6 mg/ml, BSA 0.4 mg/ml, SL 0.3 mg/ml), and Method C (TMC372 mg/ml, TPP 0.6 mg/ml, 2 mg BHb was added in TPP solution). All data are the mean ± S.D. ($n = 3$).

at the particle surface could cause the delivery system to fail. Thus, the initial burst must be controlled. Alginate modification reduced BSA burst release (Fig. 7), probably by forming a polyelectrolyte complex layer on the particle surface with cationic polysaccharides (Shu and Zhu, 2000). Therefore, less BSA was gelated with TMC due to the competition with SL (the similarity of the structures of TMC and SL makes it more likely than BSA to cross-link with TMC). Although the burst release was reduced from 60% to 45% (SL 0.3 mg/ml) and a lower burst release was observed as the SL concentration increased, the result was still not satisfactory. This was probably because of a relatively low SL/TMC ratio (w/w, 3/50) in our experiment. A better result was observed with a much higher SL/cationic polysaccharides polymer ratio (w/w, 1/4) (Xu et al., 2003). However, in our experiment too high a ratio (>1/10) would lead to aggregation, as mentioned above.

Burst release was not increased by increasing the loading efficiency of BHb-loaded nanoparticles prepared by Method C (Fig. 7), indicating that this method did not lead to an increase of BHb bound to TMC on the nanoparticle surface. The release curve was similar to that of BHb nanoparticles prepared by Method A.

4. Conclusion

In our study, *N*-trimethyl chitosan chloride nanoparticles were prepared by ionic cross-linking with TPP. A small particle size and a positive zeta potential were observed. A high loading efficiency (95%) was obtained in BSA-loaded nanoparticles prepared by TMC with either a lower (TMC33) or higher (TMC37) degree of quaternization. While only 30% of BHb was entrapped in TMC37 nanoparticles, the loading efficiency was higher in nanoparticles prepared by TMC with a lower degree of quaternization (TMC33). The poor loading efficiency can be improved from 30% to 50% by dissolving BHb in TPP to achieve a negative charge before adding it to the TMC solution. Increasing the degree of quaternization of TMC can reduce the particle size and enhance the zeta potential. The release profile of TMC nanoparticles showed a burst release followed by a sustained release. Better nanoparticle properties can be achieved and the burst release can be reduced by alginate modification. A slightly slower drug-release was obtained when nanoparticles were prepared by TMC with a lower degree of quaternization.

Acknowledgements

The research described above was supported by National Natural Science Foundation (30500636) of the People's Republic of China and Key Technological Project of Sichuan Province (04SG022-009-5).

References

Amidi, M., Romeijn, S.G., Borchard, G., Junginger, H.E., Hennink, W.E., Jiskoot, W., 2006. Preparation and characterization of protein-loaded *N*-trimethyl chitosan nanoparticles as nasal delivery system. J. Control. Rel. 111, 107–116.

Aral, C., Akbuğa, J., 1998. Alternative approach to preparation of chitosan beads. Int. J. Pharm. 168, 9–15.

Artursson, P., Lindmark, T., Davis, S.S., Illum, L., 1994. Effect of chitosan on the permeability of monolayers of intestinal epithelial cells (Caco-2). Pharm. Res. 11, 1358–1361.

Bernkop-Schurch, A., Humenberg, C., Valenta, C., 1998. Basic Studies on bioadhesive delivery systems for peptide and protein drugs. Int. J. Pharm. 165, 217–225.

Bouillot, P., Ubrich, N., Sommer, F., Duc, T.M., Loeffler, J.P., 1999. Dellacherie E. Protein encapsulation in biodegradable amphiphilic microspheres. Int. J. Pharm. 181, 159–172.

Crotts, G., Sah, H., Park, T.G., 1997. Adsorption determines in vitro protein release rate from biodegradable microspheres: quantative analysis of surface area during degradation. J. Control. Rel. 41, 101–111.

Domard, A., Rinaudo, M., Terrassin, C., 1986. New method for the quaternisation of chitosan. Int. J. Biol. Macromol. 8, 105–107.

Felt, O., Buri, P., Gurny, R., 1998. Chitosan: a unique polysaccharide for drug delivery. Drug Dev. Ind. Pharm. 24, 979–993.

González-Rodrŕguez, M.L., Holgado, M.A., Sánchez-Lafuente, C., Rabasco, A.M., Fini, A., 2002. Alginate/chitosan particulate systems for sodium diclofenac release. Int. J. Pharm. 232, 225–234.

Hamman, J.H., Stander, M., Kotzé, A.F., 2002. Effect of the degree of quaternization of *N*-trimethyl chitosan chloride on absorption enhancement: in vivo evaluation in rat nasal epithelia. Int. J. Pharm. 232, 235–242.

Issa, M.M., Köping-Höggård, M., Artursson, P., 2005. Chitosan and the mucosal delivery of biotechnology drugs. Drug Discovery Today 2, 1–6.

Kotzé, A.F., Luehen, H.L., de Leeuw, B.J., de Boer, A.G., Verhoef, J.C., Junginger, H.E., 1999. Chitosan for enhanced intestinal permeability: prospects for derivatives soluble in neutral and basic environments. Eur. J. Pharm. Sci. 7, 145–151.

Kotzé, A.F., Luehen, H.L., de Leeuw, B.J., de Boer, A.G., Verhoef, J.C., Junginger, H.E., 1997. *N*-trimethyl chitosan chloride as a potential absorption enhancer across mucosal surfaces: in vitro evaluation in intestinal epithelial cells (Caco-2). Pharm. Res. 14, 1197–1202.

Lee, K.Y., Ha, W.S., Park, W.H., 1995. Blood compatibility and biodegradability of partially N-acylated chitosan derivatives. Biomaterials 16, 1211–1216.

Onishi, H., Machida, Y., 1999. Biodegradation and distribution of water-soluble chitosan in mice. Biomaterials 20, 175–182.

Shu, X.Z., Zhu, K.J., 2000. A novel approach to prepare tripolyphosphate:chitosan complex beads for controlled release drug delivery. Int. J. Pharm. 201, 51–58.

Sieval, A.B., Thanou, M., Kotzé, A.F., Verhoef, J.C., Brussee, J., Junginger, H.E., 1998. Preparation and NMR-characterisation of highly substituted Ntrimethyl chitosan chloride. Carbohydr. Polym. 36, 157–165.

Thanou, M., Kotzé, A.F., Scharringhausen, T., Luessen, H.L., De Boer, A.G., Verhoef, J.C., Junginger, H.E., 2000. Effect of degree of quaternisation of *N*-trimethyl chitosan chloride for enhanced transport of hydrophilic compounds across intestinal Caco-2 cell monolayers. J. Control. Rel. 64, 15–25.

van der Lubben, I.M., Kersten, G., Fretz, M.M., Beuvery, C., Verhoef, J.C., Junginger, H.E., 2003. Chitosan microparticles for mucosal vaccination against diphtheria: oral and nasal efficacy studies in mice. Vaccine 28, 1400–1408.

van der Lubben, I.M., Verhoef, J.C., Borchard, G., Junginger, H.E., 2001. Chitosan for mucosal vaccination. Adv. Drug Deliv. Rev. 52, 139–144.

van der Merwe, S.M., Verhoef, J.C., Verheijden, J.H.M., Kotzé, A.F., Junginger, H.E., 2004a. Trimethylated chitosan as polymeric absorption enhancer for improved peroral delivery of peptide drugs. Eur. J. Pharm. Biopharm. 58, 225–235.

van der Merwe, S.M., Verhoef, J.C., Kotzé, A.F., Junginger, H.E., 2004b. *N*-Trimethyl chitosan chloride as absorption enhancer in oral peptide drug delivery. Development and characterization of minitablet and granule formulations. Eur. J. Pharm. Biopharm. 57, 85–91.

Vandenberg, G.W., Drolet, C., Scott, S.L., de la Noüe, J., 2001. Factors affecting protein release from alginate-chitosan coacervate microcapsules during production and gastric/intestinal simulation. J. Control. Rel. 77, 297–307.

Xu, Y., Du, Y., Huang, R., Gao, L., 2003. Preparation and modification of N-(2-hydroxyl) propyl-3-trimethyl ammonium chitosan chloride nanoparticle as a protein carrier. Biomaterials 24, 5015–5022.